Evolution of a Digital Twin for Wing Assembly by Refill Friction Stir Spot Welding

Johnathon Hunt[1], Thomas Richardson[2], and Yuri Hovanski[3]

***Abstract*— Refill Friction Stir Spot Welding (RFSSW) is an emerging solid state joining process for thin sheet aluminum. Many researchers are developing RFSSW process parameters and best practices for manufacturing, thus enabling the use of RFSSW in many industries. Within this development, this work focuses to predict the resultant residual stresses and distortion in a joined part after welding. These residual stresses are caused by the heat & mechanical inputs from the RFSSW process. This report provides the preliminary results of the two step solution to resultant temperature and stresses from a series of RFSSW in thin sheet aluminum.**

I. INTRODUCTION

Refill friction stir spot welding (RFSSW) is a solid-state joining process that uses heat, produced by friction, and mechanical inputs to join two materials. Recently, RFSSW has shown potential in joining thin sheet aluminum for the aerospace industry. RFSSW does not introduce holes that rivets currently occupy and they do not increase the weight of the part as workpieces become the joint, unlike rivets or bolts. RFSSW is an emerging technology, and many are exploring RFSSW properties and performance to enable its use in industry [1, 2]. However, in many research environments usually a single RFSSW is examined; when in an aerospace application RFSSW would be used in much larger quantities to manufacture wing components or other parts. Thus, an understanding of single weld, as well as, multiple weld properties will be need to empower the use of RFSSW in industry.

Creating large amounts of experimental data and the analysis of that data becomes costly because of the material cost as well as the time needed to preform such an exhaustive study. To reduce the time and cost of this endeavor a digital twin of the RFSSW process for 10 spot welds is being developed in ANSYS. The model will provide temperature, residual stress and distortion predictions that will be used to inform manufacturers what is the best order to preform weldments to minimize distortion and residual stresses. This work provides a summary of the preliminary results of the development of this digital twin.

[1]Johnathon Hunt is a graduate student in the Department of Mechanical Engineering, Brigham Young University john.hunt@byu.edu

[2]Thomas Richardson is an undergraduate in the Department of Mechanical Engineering, Brigham Young University thomaser@byu.edu

[3]Yuri Hovanski is a professor in the Department of Manufacturing Engineering, Brigham Young University yuri.hovanski@byu.edu

A. *Background*

RFSSW was invented in the early 2000 and due to the potential benefits in manufacturing large amounts of research are being conducted to enable the use if RFSSW in industry. The process uses a 3-piece tool set as seen in Fig. 1, to create frictional heat and pressure in the workpiece to create material flow and a bond between two sheets.

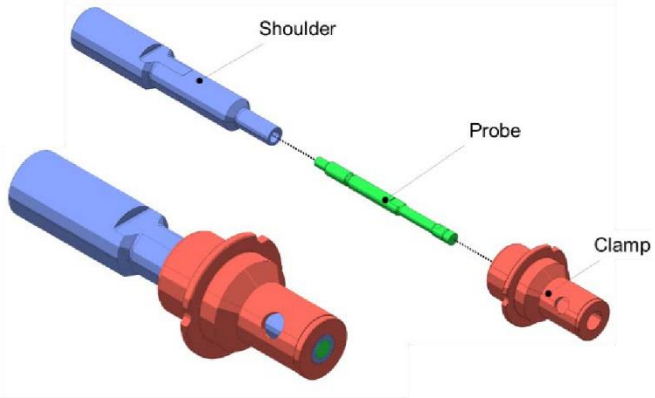

Fig. 1: The three different pieces of a RFSSW tools set: the shoulder, probe, and clamp.

The RFSSW tool sequence often includes four stages: preheating, plunging, dwelling, and refilling as shown in Fig. 2.

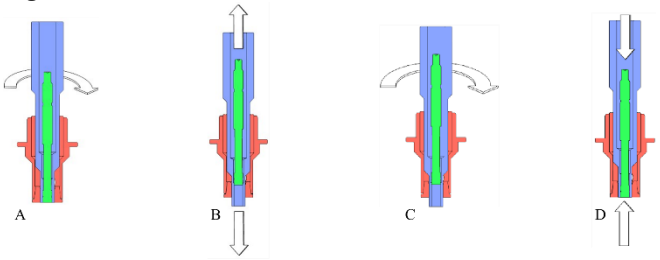

Fig. 2: The four common stages in RFSSW. A) Demonstrates the preheating at the start of the weld with the material clamped in place with the probe and shoulder rotating at the surface of the material. B) Illustrates the plunge

where the shoulder plunges into the material and the probe raises mechanically displacing the material. C) Conveys the dwell of the plunge movement allowing additional time for the material to flow. D) Shows the probe pushing the material flush to the top of the workpiece.

For the experimental welds used in this study no preheat or dwell stages were apart of the welding process, only a plunge and refill stages were included.

B. RFSSW in manufacturing

Joining large parts together via welding creates residual stresses and distortion caused from heat inputs and the constraints that the weld imposes [3, 4]. These two factors can affect the strength, fatigue, and fracture properties which are crucial in the aerospace industry.

II. METHODOLOGY

A. Experiment Setup

Material & Tools. Aluminum alloy (AA) 7075-T6 sheet metal was sheared into coupons to manufacture single a RFSSW. The composition of this allow is found in Table 1. The coupons were 25.4 x 76.2 x 1.58 mm. One coupon was placed on top of another coupon in a "lap weld" configuration with 25.4 mm overlap as seen in Fig. 33. A spacer coupon was place beneath the top coupon to keep the top coupon level.

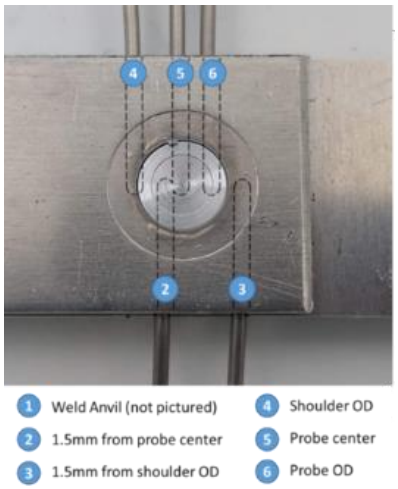

Fig. 3: The locations of the thermocouples in the single spot weld experiments.

All welds were naturally aged for 96 hrs. Then cross sections were polished and imaged to ensure that the welds were defect free and desirable joints.

Steel tooling made from heat treated H13 tool steel were used for the probe, shoulder and clamp as seen in Fig. 4. The anvil directly underneath the weld is a circular polycrystalline diamond (PCD) layer grown on top of a tungsten carbide (WC) puck. The coupons rest on an aluminum base where the anvil resides in the center of the base directly underneath the RFSSW tooling.

TABLE 1: The composition of AA 7075-T6.

Weight%	7075 min	7075 max
Al	Rem	Rem
Si	-	0.4
Fe	-	0.5
Cu	1.2	2
Mn	-	0.3
Mg	2.1	2.9
Cr	0.18	0.28
Zn	5.1	6.1
Ti	-	0.2
Other Each	-	0.05
Others Total	-	0.15

The plunge sequence included a two-stage plunge starting with the shoulder plunging at 225 mm/min to a depth of -1.5 mm from the top of the top coupon into the material. Then the shoulder continued its plunge at 120 mm/min until it reached -2 mm. During the plunge, the probe also had a two-step process. First, the probe raised at a height of 3.63 mm at 545 mm/min and then raised to 4.23 mm at 144 mm/min. The refill stage included the probe pushing the material back to a depth of -4.43 mm from its peak height at 760 mm/min. Simultaneously the shoulder raised back up 2 mm from its lowest point at 325 mm/min. Note that the refill stage finishes with the probe 0.2 mm lower than the initial starting plane. This addition of force at the end of the weld ensures that the weld is free of defects that the plunge may have introduced. Through out the entire weld the probe and shoulder spindle speed were 2600 RPM.

Fig. 4: RFSSW tools and anvil.

Temperature data was measures in 5 locations across the weld diameter as shown in Fig. 3. These temperatures were measured by k type thermocouples which were tied into the native DAC systems on the welding machine. Temperatures were measured at 1 Hz.

Machine. Single spot welds were manufactured on the BYU campus BOND RFSSW machine combined with a B&R controller. Specifications and machine capabilities are found in TABLE 2. For single coupon welds no external material clamps were used. Dowel pins aligned the two coupons to ensure they were parallel to each other.

TABLE 2: BOND RFSSW machine specifications and capabilities.

Max Spindle RPM	6000 RPM
Max Vertical Feed Rate	3000 mm/min
Max Downforce	30 kN
Clamping Force	Variable (9 kN max)
Max Torque Capability	48 N-m
Weight	72 kg

Program. Development of the digital twin was performed with ANSYS Workbench 2020 R1. The computer used to run the simulations included 16 gigabits of RAM with a 3.2 GHz processor.

B. Model

Temperature dependent properties including yield strength, Young's Modulus, density, specific heat and thermal conductivity [5-8] were the first inputs to the ANSYS model. Next the geometry was built in the native computer aided design (CAD) package in ANSYS 2020 R1 workbench. The workpiece was split into four sperate volumes. First, at the center of the overlap a cylinder with the diameter and height equal to the RFSSW kinematics volume of the probe during welding was created. Then a ring around the probe volume matching the volume of the shoulder kinematics was added. Another ring with the dimensions of the clamp with a 0.1 mm height was created. Last, the rest of the coupons volume were added to the geometry. Mesh sizes and time steps varied throughout the development of the model. The model was a two-step process, first, a transient thermal solution is found with the appropriate boundary and initial conditions. This solution was then used as an input to a transient structural tool which would solve for the Von Mises Stress and displacement. It is worth noting that the goal of this work is to predict distortion of higher number of consecutive RFSSWs which disqualifies the use of symmetry in the weldment. A complete model is necessary to predict extreme displacement and include consecutive weld consequences.

Proof of Concept. To start the development of a digital twin for RFSSW in AA 7075-T6, a simple model was created to verify the two-step process to solve for temperature and stresses and displacements. This model included two sheets lap welded with all 10 spot welds. The temperature boundary and initial conditions included: A constant temperature at 350 degrees Celsius as an input for one second within the probe volume. A convection heat transfer equilibrium at all open surfaces. No conduction boundary conditions were used in this initial effort. This problem solved for temperature profiles for 10 seconds total including the initial second of temperature input.

The transient structural tool then used the temperature profile to solve for residual stresses. The top and bottom of the open faces were constrained in the Z direction. Von Mises Stress was then calculated for 10 seconds corresponding to the temperature profile.

Single Spot Weld. After the initial proof of concept for the two-step solution in ANSYS the authors focused on validating the model to the experimental single spot weld temperature data. To start this representative model the authors created a thermal resistive circuit to solve for the heat transfer rate. This heat rate would be used as an input to the transient thermal solution. The basic equation to solve for this heat rate is found in equation 1. The change in temperature ranged from room temperature to the maximum temperature in the single spot weld.

$$q = \frac{\Delta T}{R_T} \qquad (1)$$

The total thermal resistance included the coupons and external clamping for the sheets as shown in Fig. 5. Contact resistances for aluminum to aluminum interfaces with air in between them were taken from heat transfer literature [9, 10]. Heat rates were then solved across the variable thermal resistances due to the varying temperature differences. The change in temperature changes affected the thermal conductivity of the clamp rods which slightly changed the

overall thermal resistance. The relationship between the heat rate and the change in temperature can be seen Fig. 6:.

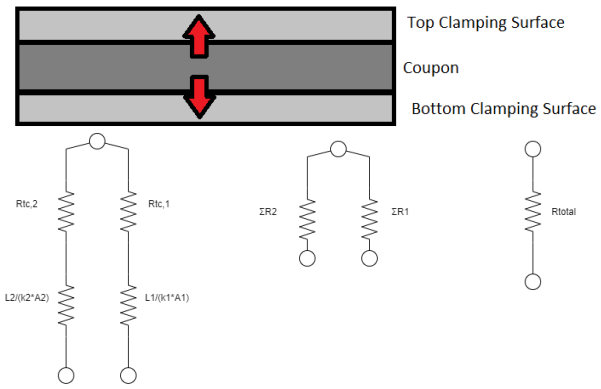

Fig. 5: The thermal resistance model for the RFSSW welding scenario.

Any open faces were defined with a free convection boundary condition. The free convection coefficient was calculated by equation 2 [9].

$$h = 0.54 \frac{k_{air} g \beta (T_{sur} - T_{\infty}) L^2}{\nu^2} Pr \qquad (2)$$

Coefficient values were calculated for surface temperatures from 21 degrees Celsius to 180 degrees Celsius as defined by the experimental data 1.5 mm from the outside diameter of the shoulder. The initial conditions of the plates were room temperature for all sheets. Finally, the probe volume was defined as a constant surface temperature of 375 degrees Celsius for the first second of solution time. Due to the fast cycle time of the weld a constant temperature was more representative than attempting to model the variable heat transfer caused from the mechanical and frictional heat input during welding. An ANSYS mesh size of 2, with multizone meshing enabled to give a finer zone at the center of the welds and courser mesh further away from center, was used in this simultion. The time step was set to one hundredth of second for the first second, thus enabling the ability to track the temperature rise during the weld time. This time step allowed high enough fidelity to compare the predicted temperature to the experimental data. Then the time step was adjusted to one second thereafter with a total time of 30 seconds. With these boundaries and initial conditions, a transient thermal solution could then be passed into a transient structural problem.

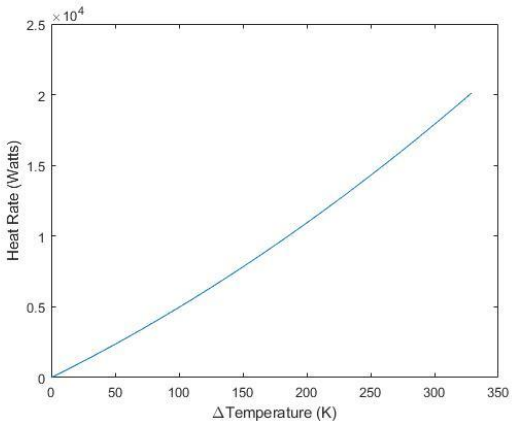

Fig. 6: Heat rate for conduction as a function of change in temperature for the RFSSW process.

The transient structural boundary conditions included the probe, shoulder, and clamp force profiles from the experimental data. At the second time step a constraint in the z direction was added to the part to replicate the weld. The solution solved for the same 30 second time similar to the transient thermal solution.

Three RFSSW. Once the single weld temperature profile was validated with the experimental data, the authors increased the geometric fidelity by creating a 3-spot weld with the same boundary and initial conditions, time frame, material properties and force profiles as the single spot weld configuration, except for a longer solution time of 65 seconds.

After solving the 3-spot weld configuration and comparing it to the single weld configuration the addition of external clamping was added to the single weld geometry. This clamping constrained the coupons in all three cartesian coordinate directions as shown in Fig. 7. The clamping conditions were then added to the 3-spot weld configuration.

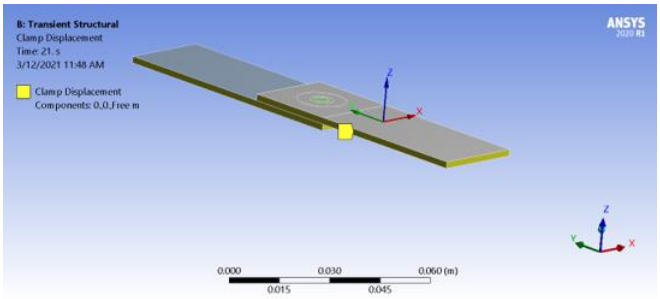

Fig. 7: An image of the clamping constraints on the single spot weld geometry.

III. RESULTS & DISCUSSION

The simulations of the single weld and 3-spot weld provided predicted values of both temperature and residual stresses from the RFSSW process. These results are preliminary that are currently advancing the development of the RFSSW digital twin.

A. Proof of Concept.

At the beginning of this work a proof-of-concept model was run to verify that the thermal solution would be correctly passed through to the transient structural model. The model was successful in calculating a solution, and the stress results are in Fig. 8. The predicted stresses range from 7 MPa to 931 MPa. The runtime for this simulation was 3.5 hours. This solution confirmed that the structure of the ANSYS model was functioning correctly and that higher fidelity details could be added to model.

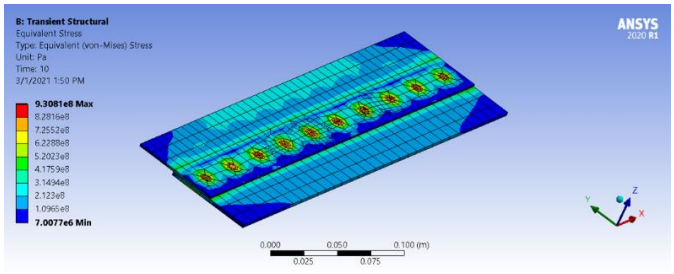

Fig. 8: Ten-spot weld proof of concept model to indicate proper passing thermal data into a transient structural tool in order to solve stresses and displacements.

B. Single Spot Weld

The experimental temperatures that validated the single spot weld configuration is found in Fig. 9. The highest temperatures are found at the center of the welds where thermocouples 2 and 5 were placed in Fig. 3. The maximum temperature is 366 degrees Celsius at 0.58 seconds into the weld. The ANSYS model's maximum temperature at the bottom of the probe volume is found in Fig. 10.

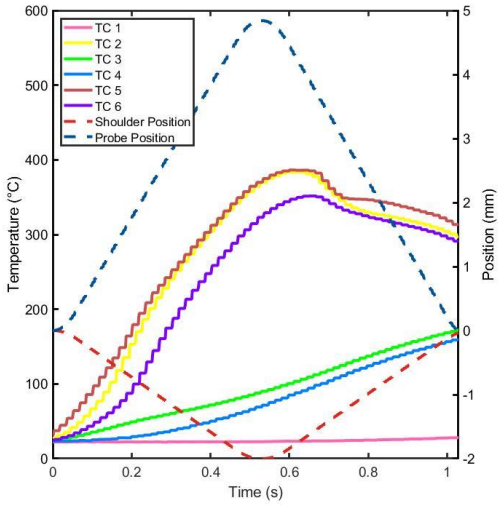

Fig. 9: An example plot of temperature from 5 different locations in a RFSSW used to validate the single spot weld configuration.

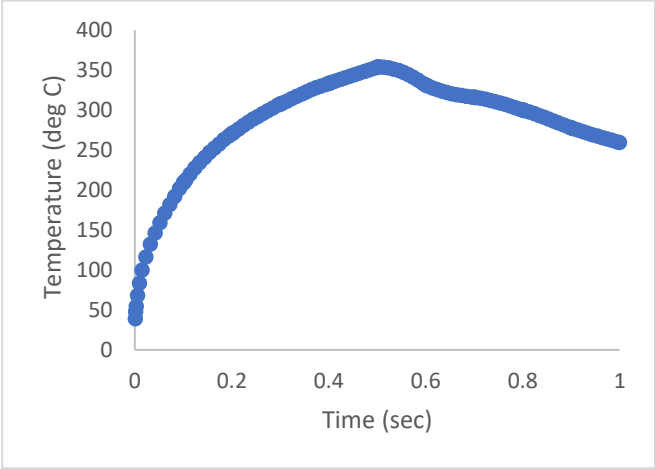

Fig. 10: The temperature at the center point directly beneath the probe volume of the ANSYS single weld configuration model.

The ANSYS model predicted a maximum temperature of 354 degrees Celsius at 0. 52 seconds into the weld, 3.27% error. After the maximum temperature, the model follows a similar cooling rate as the actual temperature of the coupon. However, the rise in temperature during the first 0.2 seconds of the weld does not match the experimental curve. The experimental curve follows a parabolic nature while the ANSYS model follows an exponential nature. This discrepancy only occurs in the first 0.2 seconds of the weld and can be assumed to have negligible affects in the overall

stress and displacement results. Von Mises stress values of the single weld configuration is found in **Error! Reference source not found.**. The stress ranges from 1.1 MPa to 10.2 MPa. Currently, no validation of the stress or displacement values has been addressed and will be a large focus in future work of this project. Lastly the runtime for the single spot weld configuration for the 30 second time took 3.2 hours.

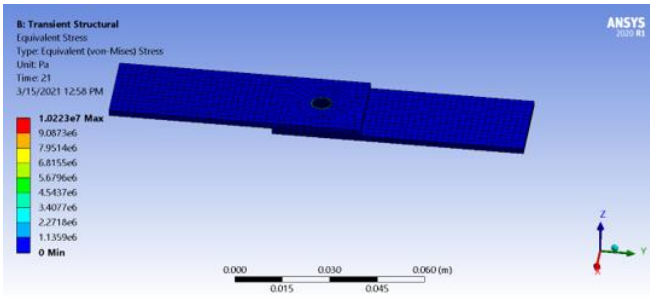

Fig. 11: The Von Mises Stress solution for the single spot weld configuration.

C. *Three RFSSW*

After the single spot weld configuration was validated, the authors focused on building a model that better represented the consequence of multiple spot welds. Thus a 3-spot weld ANSYS model was built with the same boundary conditions and other inputs as the single spot weld configuration was developed. The author's hypothesized that the temperatures and stresses would be similar to the single spot weld configuration, if not higher; and that development on a full ten spot weld could be executed. However, the temperatures in the 3-spot weld model did not match the experimental data as shown in Fig. 12. The range of temperature in this image is from 22 degrees Celsius to 301 degree Celsius. The maximum temperature is about 65 degrees lower than the experimental data. This discrepancy discourages the continuation to a 10-spot weld configuration. With three heat inputs the maximum workpiece temperature that the model predicts should be higher than the single spot weld configuration. This would be caused by the heat saturation of the workpieces by the heat input and the slow heat transfer with a free convection boundary condition. However, the predicted maximum temperature is lower than the maximum temperature of the single weld configuration. Possible solutions to make the model more representative would be to analyze the conduction heat transfer values to check to see if excessive heat transfer is passed into the clamp bars. Another possible solution would be to verify that the rate of the free convection heat transfer values to ensure they are not too high. Lastly, the time step configuration could attribute to the solution's stability. Analyzing these three model characteristics will be the next steps in building an accurate digital twin to the RFSSW process.

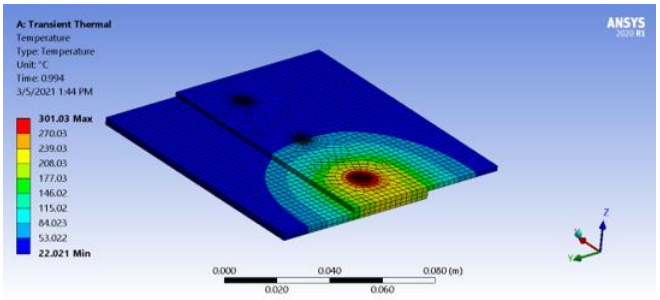

Fig. 12: The temperature distribution for the 3-spot weld configuration.

The resultant stress solution is shown in Fig. 13. The range of stresses range from 2.4 MPa to 555 MPa. These stresses are an order of magnitude larger than the single spot weld configuration. As noted above currently no validation of the displacement or stress have been possible. Thus, no main conclusions can be made from the transient structural solution. However, the authors believe the predicted stresses may be an exaggeration of the actual stresses in a 3-spot weld configuration since the predictions are an order of magnitude greater than the single spot weld configuration and the predicted temperatures are not accurate which would affect the accuracy of the predicted stresses.

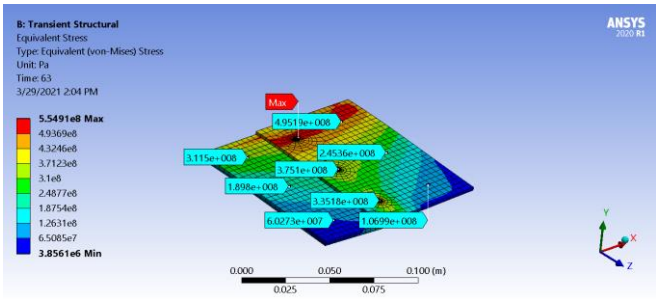

Fig. 13: The solution for the Von Mises Stress for the 3-spot weld configuration.

IV. CONCLUSIONS & FUTURE WORK

A. *Conclusions*

As introduced, this work provides the preliminary work to model and predict the residual stresses that occur from a series of RFSSW. Currently single spot weld ANSYS models provide accurate temperature predictions with under 5% error. However, when the same conditions are used for a 3-spot weld the predicted temperature has 18% error.

B. *Future Work*

To continue this work validation of the 3-spot weld will be performed. This validation will include additional analysis for the free convection boundary conditions as well as the heat

transfer rate of conduction between the clamping workpieces. Additionally, the time step will be examined to ensure all solutions are stable. Once the 3-spot weld predicted temperature have been validated then a 10-spot weld configuration will be developed, and the predicted temperatures will be validated. 10-spot weld configuration panels will then be manufactured, and displacement will be measured and compared to the predicted displacement to complete the digital twin model. With the displacements validated variations of weld order will be performed and to predict which will result in the least amount of residual stress and distortion.

REFERENCES

[1] B Larsen and Y Hovanski, "Reducing Cycle Times of Refill Friction Stir Spot Welding in Automotive Aluminum Alloys," SAE Technical Paper, 0148-7191, 2020.

[2] Y Hovanski, B Larsen, B Carlson, and R Szymanski, (2018) Initial Comparisons of Friction Stir Spot Welding and Self Piercing Riveting of Ultra-Thin Steel Sheet. [Online]. Available: https://doi.org/10.4271/2018-01-1236.

[3] MA Sutton , AP Reynolds, D-Q Wang , and CR Hubbard, (2002) A Study of Residual Stresses and Microstructure in 2024-T3 Aluminum Friction Stir Butt Welds *Journal of Engineering Materials and Technology* **124**(2):215-221 doi: 10.1115/1.1429639 %J Journal of Engineering Materials and Technology.

[4] G Bussu and PE Irving, (2003) The role of residual stress and heat affected zone properties on fatigue crack propagation in friction stir welded 2024-T351 aluminium joints *International Journal of Fatigue* **25**(1):77-88 doi: https://doi.org/10.1016/S0142-1123(02)00038-5.

[5] Kethireddy Narender, Ammiraju Sowbhagya Madhusudhan Rao, Kalvala Gopal Kishan Rao, and NG Krishna, (2013) Temperature Dependence of Density and Thermal Expansion of Wrought Aluminum Alloys 7041, 7075 and 7095 by Gamma Ray Attenuation Method *Journal of Modern Physics* **4**(3):331-336 doi: 10.4236/jmp.2013.43045.

[6] P. Jeanmart and J Bouvaist, (1985) Finite element calculation and measurement of thermal stresses in quenched plates of high–strength 7075 aluminium alloy *Mater Sci Tech Ser* **1**(10):765 doi: 10.1179/mst.1985.1.10.765..

[7] K Senthil, MA Iqbal, PS Chandel, and NK Gupta, (2017) Study of the constitutive behavior of 7075-T651 aluminum alloy *International Journal of Impact Engineering* **108**(171-190 doi: https://doi.org/10.1016/j.ijimpeng.2017.05.002..

[8] JG Kaufman, (1999) Properties of Aluminum Alloys: Tensile, Creep and Fatigue Data at High and Low Temperatures.

[9] TL Bergman, FP Incropera, DP DeWitt, and AS Lavine, (2011) Fundamentals of heat and mass transfer.

[10] DW Hahn and MN Özisik, (2012) Heat conduction.